Length Scales at which Classical Elasticity Breaks Down for Various Materials

R. Maranganti and P. Sharma*

Department of Mechanical Engineering, University of Houston, Houston, Texas 77204
and Department of Physics, University of Houston, Houston, Texas 77204, USA

(Received 7 February 2007; published 9 May 2007; corrected 11 May 2007)

At what characteristic length scale does classical continuum elasticity cease to accurately describe small deformation mechanical behavior? The two dominant physical mechanisms that lead to size dependency of elastic behavior at the nanoscale are surface energy effects and nonlocal interactions. The latter arises due to the discrete structure of matter and the fluctuations in the interatomic forces that are smeared out within the phenomenological elastic modulus at coarser sizes. While surface energy effects have been well characterized in the literature, little is known about the length scales at which nonlocal effects manifest for different materials. Using a combination of empirical molecular dynamics and lattice dynamics (empirical and *ab initio*), we provide estimates of nonlocal elasticity length scales for various classes of materials: semiconductors, metals, amorphous solids, and polymers.

DOI: 10.1103/PhysRevLett.98.195504 PACS numbers: 62.25.+g, 62.20.Dc

Classical elasticity is inherently size independent. Most materials exhibit size-dependent elastic phenomena in the length scale range of 1–10 nm due to surface energy effects which become increasingly appreciable due to the large surface-to-volume ratios available at the nanoscale [1–3]. However, nonlocality of the stress-strain relationship introduces yet another length scale at which classical elasticity breaks down. A fundamental notion of classical continuum elasticity is that the length scale over which deformation varies is much larger than the discrete length of the matter. This argument would set the breakdown length scale to be in the region of the lattice parameter for most materials. However, discreteness is not the only cause of nonlocality. Long-ranged nature of interatomic forces (say in polar materials) also results in a nonlocal stress-strain relationship. Further, fluctuations in interatomic forces (say, for example, in amorphous solids) can result in large nonaffine displacement fields upon deformation. The characteristic length scale over which the nonaffine field is correlated serves as a lower limit beyond which classical continuum elasticity cannot be applied [4]. Thus, an assessment of the validity of classical elasticity must figure in accurate interatomic behavior.

The nonlocal stress-strain behavior can be mimicked in a continuum fashion by including strain-gradient terms in addition to the classical terms in the linearized elastic Lagrangian as shown in Eq. (1) [5–7]

$$L = \frac{1}{2}\rho \dot{u}_i \dot{u}_i - \frac{1}{2} C_{ijkl} e_{ij} e_{kl} - D_{ijklm} u_{i,j} u_{k,lm} - F^1_{ijklmn} u_{i,jk} u_{l,mn} - F^2_{ijklmn} e_{ij} u_{k,lmn}. \quad (1)$$

ρ is the mass density of the solid, $\mathbf{u}$ is the displacement field; the dot on top of u_i denotes differentiation with respect to time, and the commas denotes differentiation with respect to the spatial variables in the reference configuration. $\mathbf{e}$ is the symmetric strain tensor. While $\mathbf{C}$ in Eq. (1) represents the well-known elastic modulus tensor, $\mathbf{D}$, $\mathbf{F}^1$, and $\mathbf{F}^2$ are the newly introduced strain-gradient elastic moduli. At larger length scales (assuming small deformations and rotations), the term involving $\mathbf{C}$ dominates the potential energy, and the higher-order gradient terms involving the coefficients $\mathbf{D}$, $\mathbf{F}^1$, and $\mathbf{F}^2$ provide negligible contributions. However, in the presence of large strain gradients, the contributions due to these higher-order terms may prove to be significant and is in fact the *raison d' etre* for this theory [8].

From the equations of motion obtained from the Lagrangian of Eq. (1), the dispersion law for $\omega(\mathbf{k})$ (frequency ω vs wave vector $\mathbf{k}$ relation for acoustic waves) can be written as Eq. (2) below:

$$\rho\omega^2 u^0_i = \begin{pmatrix} c_{ijkl}k_j k_l + i d_{ijklm} k_j k_l k_m \\ -f_{ijklmn} k_j k_l k_m k_n \end{pmatrix} u^0_k \quad (2)$$

Constants $\mathbf{c}$, $\mathbf{d}$, and $\mathbf{f}$ are called the dynamic elastic constants and are related to their static counterparts by a set of noninvertible equations Eqs. (3)–(5).

$$c_{ijkl} = \mathrm{sym}_{(i,k)}\mathrm{sym}_{(j,l)} C_{ijkl} \quad (3)$$

$$d_{ijklm} = \mathrm{asym}_{(i,k)}\mathrm{sym}_{(j,l,m)} D_{ijklm} \quad (4)$$

$$f_{ijklmn} = \mathrm{sym}_{(i,k)}\mathrm{sym}_{(j,l,m,n)}(F^2_{ijklmn} - F^1_{ijlkmn}) \quad (5)$$

The symbols "sym" and "asym," respectively, denote symmetrization and antisymmetrization with respect to the indices in the subscripts. A group-theoretical analysis to determine the number of independent components of tensors $\mathbf{c}$, $\mathbf{d}$, and $\mathbf{f}$ for crystals possessing point-group symmetry $43m$ (corresponding to a zinc-blende like crystal: say GaAs) has already been carried out by Divincenzo [6]. The classical dynamical elastic constant $\mathbf{c}$ has three independent components c_{1111}, c_{1212}, and c_{1122}; the fifth-order tensor $\mathbf{d}$ possesses only one, d_{12223}, while the sixth-order tensor $\mathbf{f}$ has six independent components. For centrosymmetric crystals such as the silicon (Si) and fcc copper (Cu),

the odd-order tensor **d** vanishes. Further, under isotropy, these constants satisfy additional constraints [9] such that only two independent components of **c** and **f** remain. Now, following Eq. (2), the isotropic dispersion relations corresponding to the longitudinal and acoustic modes along $\mathbf{k} = [100]$ take the form $\rho\omega^2 = ck^2 - fk^4$ from which two isotropic nonlocal length scale parameters $l_1 = \sqrt{f_{111111}/c_{1111}}$ and $l_2 = \sqrt{f_{122122}/c_{1212}}$ can be identified. Quantification of these intrinsic length parameters provides a measure of the length scale at which it is no longer accurate to use classical elasticity (which corresponds to $l_1 = l_2 = 0$). At present, very little work exists on the evaluation of these lengths, and certainly no clear consensus exists on their variation for various groups of materials and the reasons for why certain materials may possess higher length scales than others.

Equation (2) represents the phonon dispersion relations predicted by our extended continuum elasticity theory and can be written as Eq. (6) below:

$$\rho\omega^2 u_i^0 = R_{ik}(\mathbf{k}) u_k^0 \tag{6}$$

$R(\mathbf{k})$ is the dynamical matrix derived in a purely elastic continuum framework. In the absence of **d** and **f** from Eq. (2), the relationship between ω and **k** would be linear. The terms involving **d** and **f** in Eq. (2) provide a dispersive correction to this linear relationship. Measuring this dispersion can provide an estimate of these nonlocal dispersive constants. Thus, one could, in principle, generate phonon dispersion curves for various materials from either empirical or *ab initio* lattice-dynamics and estimate the values of the independent components of tensors **d** and **f**. However, the identification between the 3×3 dynamical matrix obtained via continuum nonlocal elasticity Eq. (6) and the discrete $3N \times 3N$ dynamical matrix obtained by empirical or *ab initio* lattice-dynamics techniques (N being the number of atoms in the unit cell) is not readily apparent [6]. The $3N \times 3N$ dynamical matrix obtained by discrete means needs to be block diagonalized, and its 3×3 acoustic sub-block can be identified with the 3×3 continuum dynamical matrix of Eq. (6); the components of the tensors **c**, **d**, and **f** can be subsequently isolated and the nonlocal length scales can be extracted. While this can be achieved analytically for empirical lattice dynamical models [6], the analogous procedure for *ab initio* lattice dynamics has to proceed numerically. The details involved will be discussed in a subsequent publication [10]. Figure 1 shows the phonon dispersion curves predicted by classical elasticity, nonlocal elasticity, and those generated by *ab initio* techniques for copper. It can be seen that nonlocal elasticity can model the dispersion behavior much better than classical elasticity.

Lattice-dynamics based procedures cannot be employed to extract the nonlocal length scale parameters of materials possessing a nonhomogeneous microstructure such as amorphous solids and polymers. In a classical paper by

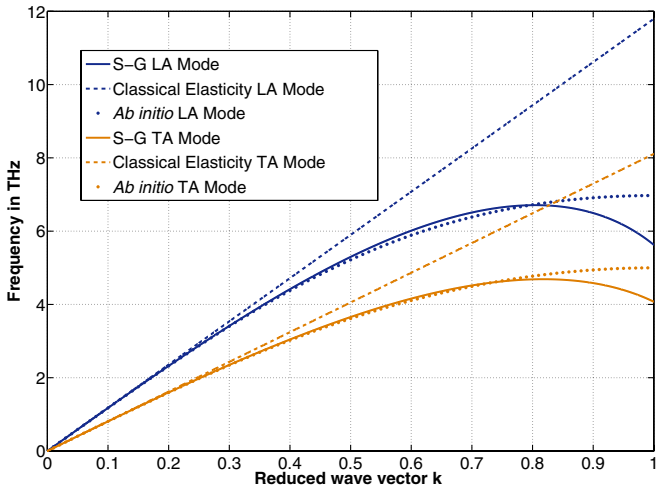

FIG. 1 (color online). Shows the comparison of phonon dispersion curves of copper (Cu) predicted by strain-gradient elasticity (S-G modes) and classical elasticity to those obtained by ab initio calculations for the transverse acoustic (TA) and longitudinal acoustic (LA) modes along $\mathbf{k} = [100]$.

Parrinello and Rahman [11], it was shown that the fluctuations in elastic strain in an (σ, H, N) ensemble (constant stress σ, constant enthalpy H, and constant number of particles N) are a direct measure of the elastic compliances in a general anisotropic medium. More recently, Meyers *et al.* [12] (based on Landau and Lifshitz [13] and Pratt [14]) have proposed a methodology to determine the classical elastic moduli from the atomic displacement correlation function in an NVT (constant number of particles N, constant volume V and constant temperature T) molecular dynamics (MD) ensemble using the long-wavelength approximation. We have extended this technique to be applicable in regime of relatively high-energy wave vectors so that the dispersive elastic constants can also be extracted from the displacement correlation functions [details to be published in a subsequent publication, Ref. [10]]. This method proves advantageous over methods involving strain-strain fluctuations (or stress-stress fluctuations) in that it involves atomic displacements which are easily determined during the course of a simulation as opposed to local strain and stress measures. Our derivations indicate that if an NVT MD simulation is carried out in a cubic simulation box with an edge of length L, then the thermal average of the displacement correlations can be related to the dynamic elastic constants as [10]

$$\langle \tilde{u}_i(\mathbf{k}) \tilde{u}_k(-\mathbf{k}) \rangle = \frac{k_B T}{L^3} \begin{pmatrix} c_{ijkl} k_j k_l + i d_{ijklm} k_j k_l k_m \\ -f_{ijklmn} k_j k_l k_m k_n \end{pmatrix}^{-1}. \tag{7}$$

k_B is the Boltzmann constant. To obtain the requisite dynamic elastic constants from Eq. (7), an NVT MD simulation is carried out at low temperature (50 K) for atoms enclosed in a cubic simulation box. The displacements of all the atoms are obtained at each time step. These

displacements in real space can be discrete Fourier-transformed, and the correlations given by the left hand side of Eq. (7) can be calculated for wave vectors along high-symmetry directions. The thermal average of the displacement correlations can be obtained for different **k**-vectors and can be numerically fitted (by a nonlinear least square minimizing technique) to the right hand side of Eq. (7) to obtain the dynamic elastic constants **c**, **d**, and **f**. In this Letter, we have used the three methods described above, namely, empirical lattice dynamics, *ab initio* lattice dynamics [15], and empirical *NVT* MD [16] to determine the dispersive elastic constants and the associated nonlocal length scales. For fcc metals Cu and Al, we have employed both *ab initio* lattice dynamics and our fluctuations-based empirical MD simulation method. For Si, we have employed all the three methods, i.e., *ab initio* and empirical lattice dynamics and empirical MD. For C (diamond) and GaAs, we have used *ab initio* and empirical lattice dynamics to estimate the dispersive constants while for Ge and GaP, we have used only empirical lattice dynamics. Lastly, for the noncrystalline systems investigated, viz., amorphous silica and polythene, only our fluctuations-based MD method is applicable. *Ab initio* phonon dispersions of Cu and diamond (*C*) were calculated within density-functional perturbation theory in the generalized gradient approximation (GGA). An ultrasoft pseudopotential generated by Favot and Dal Carso [17] using an approach outlined by Kresse and Hafner [18] was employed. *Ab initio* phonon dispersions of Al and Si were calculated in the GGA using a norm-conserving pseudopotential generated by Favot and Dal Carso [17], while those of GaAs were calculated in the Local Density Approximation (LDA) using a norm-conserving pseudopotential generated by Giannozzi *et al.* [19]. For empirical lattice dynamics, Shell Model parameters for Si, Ge, and C provided by Price *et al.* [20] were used. Similar parameters for GaAs and GaP were obtained from Kunc *et al.* [21]. While an embedded atom potential [22] was adopted to carry out MD simulations of the metals Cu, Al, and Ni, the Tersoff potential [23] was for the semiconductor Si and the Vashishta potential [24] was used to simulate SiO_2. Empirical MD simulations of multicomponent semiconductors like GaAs, etc., were avoided since reliable interatomic potentials are unavailable. Despite slow convergence of the elastic constants using Meyers *et al.*'s method [12] (compared to some other schemes such as in Ref. [25]), it was nevertheless employed since it is quite simple to extend this technique to include the effects of strain gradients. Including strain-gradient effects is not straightforward in other fluctuation-based techniques to calculate elastic constants: for example, the Parrinello-Rahman [11] technique uses a (σ, H, N) ensemble wherein a constant external stress is applied, and the fluctuations in the strain (which is the conjugate variable to stress) are in turn related to the classical elastic constants. Trying a similar approach to determine the strain-gradient elastic constants would re-

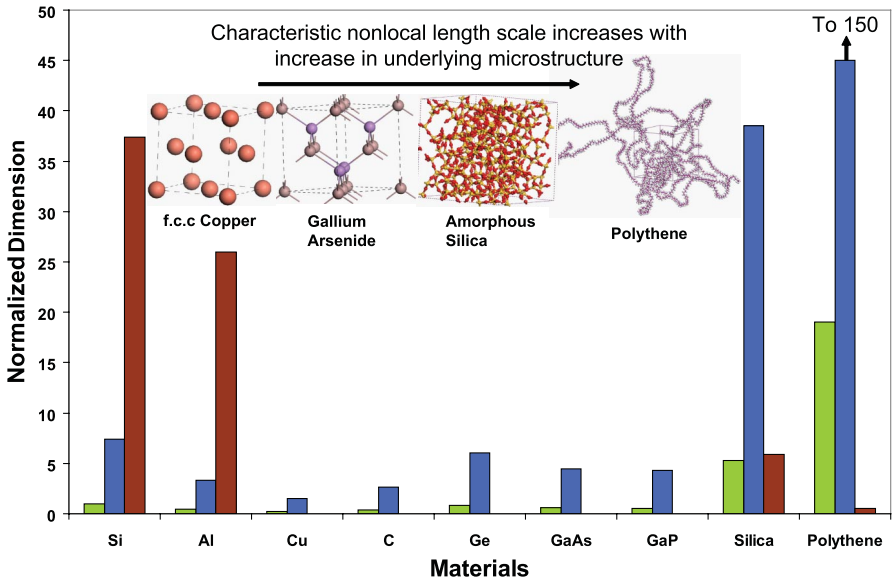

FIG. 2 (color online). In this map, some characteristic dimensions normalized with respect to the average nearest neighbor distance[26] for different materials are represented. The light bars (pale green bars in color version) represent the larger of the two isotropised nonlocal length scale parameters for different materials investigated in this work. The medium bars (blue bars in color version) represent the normalized dimension (breadth) of a beam with a square cross-section (length = 10 times the breadth) for which the size-dependent bending rigidity due to nonlocal effects differs from the bulk value by 10% as predicted by a model due to Gao *et al.* [24]. The dark bars (brown bars in color version) represent the normalized dimension (breadth) of a beam with a square cross-section for which the size-dependent bending rigidity becomes 10% higher (or 10% lower depending upon the sign of the surface elastic moduli) of the bulk value as predicted by a model incorporating surface elastic effects due to Miller and Shenoy [3].

quire application of an external "couple-stress" (conjugate variable to strain-gradient): how one can achieve this in a computational ensemble is currently unclear.

Our main results are encompassed in Fig. 2 in which we present the dimensionless nonlocal length scales (normalized with respect to the average nearest neighbor distance [26]) for different materials. Using a Bernoulli-Euler beam model predicated on strain-gradient elasticity [27], we also plot the normalized dimension (breadth) of a beam with a square cross section (length $= 10 \times$ breadth) for which the size-dependent bending rigidity due to nonlocal effects differs from the value at the bulk by 10%. As one can see, size effects will be observed in beams with dimensions as high as 30 nm for polythene and 8 nm for silica. However, for crystalline Si, the corresponding beam dimension is 1.7 nm while for Cu, it is even lower at 0.4 nm. From these results, one can infer that while nonlocal elasticity is irrelevant for most crystalline metals and semiconductors even at sizes down to a lattice parameter, it becomes important for materials possessing a nonhomogeneous microstructure like amorphous silica and polymers. In order to compare nonlocal elastic and surface energy effects in materials, we have also plotted results for beams similar to ones mentioned earlier using a model due to Miller and Shenoy [3] incorporating surface energy effects. As one can see, for crystalline systems, surface elastic effects are the dominant contributors to breakdown of classical elasticity while for amorphous systems, they are generally negligible. The high nonlocality in amorphous solids possessing an underlying inhomogenous microstructure possibly stems from a group of strongly bonded atoms behaving as a unit. Under such circumstances, parts of the material system may undergo considerable nonaffine deformation and high moment stresses may result. Liquid crystal elastomers have also been investigated under the context of Frank elasticity, and experimental evidence suggests that their length scales may lie in the 10 nm regime [28]. However, experiments on size effects on polystyrene by Stafford *et al.* [29] did not reveal any size effects down to 150 nm. A recent work by Nikolov *et al.* [30] estimated that rubbers should have nonlocal length scale in the neighborhood of 4.5 nm. Since crystalline materials are highly ordered, they very possibly undergo negligible nonaffine deformations as a consequence of which the nonlocal elastic effects are unimportant for such systems. Further, among crystalline materials, covalent semiconductors like Si tend to possess higher nonlocal length scales compared to metals which may be attributed to the short-ranged nature of interatomic forces in metals. Although our results appear to indicate that strain-gradient elasticity is irrelevant for most crystalline metals and semiconductors, we wish to point out that under certain circumstances, it is quite useful even in materials exhibiting small nonlocal characteristic length scales, e.g., in the analysis of defects in graphene [31].

Financial support from ONR Young Investigator Grant No. N000140510662 is gratefully acknowledged.

*Electronic address: psharma@uh.edu

[1] R. C. Cammarata, Prog. Surf. Sci. **46**, 1 (1994).
[2] M. E. Gurtin and A. I. Murdoch, Arch. Ration. Mech. Anal. **57**, 291 (1975).
[3] R. E. Miller and V. B. Shenoy, Nanotechnology **11**, 139 (2000).
[4] F. Leonforte, R. Boissiere, A. Tanguy, J. P. Wittmer, and J.-L. Barrat, Phys. Rev. B **72**, 224206 (2005).
[5] R. D. Mindlin, Arch. Ration. Mech. Anal. **16**, 51 (1964).
[6] D. P. DiVincenzo, Phys. Rev. B **34**, 5450 (1986).
[7] X. Zhang and P. Sharma, Phys. Rev. B **72**, 195345 (2005).
[8] We note that strain gradients are generally large only at nanoscale dimensions or in the vicinity of defects.
[9] Under isotropy, the components of tensors **c**, **d**, and **f** satisfy these relations: $2c_{1122} = c_{1111} - c_{1212}$, $d_{12223} = 0$, $f_{122133} = \frac{f_{122122}}{3}$, $f_{211222} = \frac{f_{111111}+f_{122122}}{6}$, $f_{112222} = \frac{f_{111111}-f_{122122}}{4}$, $f_{112233} = \frac{f_{111111}-f_{122122}}{12}$.
[10] R. Maranganti and P. Sharma (unpublished).
[11] M. Parrinello and A. J. Rahman, J. Chem. Phys. **76**, 2662 (1982).
[12] M. T. Meyers, J. M. Rickman, and T. J. Delph, J. Appl. Phys. **98**, 066106 (2005).
[13] L. D. Landau and E. M. Lifshitz, *Statistical Physics*, Course of Theoretical Physics Vol. 5 (Butterworth-Heinemann, Oxford, 1984), Part 1.
[14] L. R. Pratt, J. Chem. Phys. **87**, 1245 (1987).
[15] All the *ab initio* phonon calculations were done using the Quantum ESPRESSO package.
[16] All the MD simulations apart from those with polythene were carried out using GULP. Please refer to J. D. Gale, J. Chem. Soc., Faraday Trans. **93**, 629 (1997). MD simulations on polythene were carried out using Materials Studio developed by Accelyrs Inc.
[17] F. Favot and A. Dal Corso, Phys. Rev. B **60**, 11427 (1999).
[18] G. Kresse and J. Hafner, J. Phys. Condens. Matter **6**, 8245 (1994).
[19] P. Giannozzi, S. de Gironcoli, P. Pavone, and S. Baroni, Phys. Rev. B **43**, 7231 (1991).
[20] D. L. Price, J. M. Rowe, and R. M. Nicklow, Phys. Rev. B **3**, 1268 (1971).
[21] K. Kunc, M. Balkanski, and M. Nusimovici, Phys. Status Solidi B **71**, 341 (1975); **72**, 229 (1975).
[22] F. Cleri and V. Rosato, Phys. Rev. B **48**, 22 (1993).
[23] J. Tersoff, Phys. Rev. Lett. **61**, 2879 (1988).
[24] P. Vashishta, R. K. Kalia, and J. P. Rino, Phys. Rev. B **41**, 12197 (1990).
[25] J. R. Ray, M. C. Moody, and A. Rahman, Phys. Rev. B **32**, 733 (1985); **33**, 895 (1986).
[26] The average nearest neighbor distances used for different materials are Al- 2.86 Å, Si- 2.35 Å, Cu- 2.55 Å, C- 1.54 Å, Ge- 2.45 Å, GaAs- 2.44 Å, GaP- 2.35 Å, Silica- 1.7 Å, Polythene- 2 Å.
[27] S. K. Park and X.-L. Gao, J. Micromech. Microeng. **16**, 2355 (2006).
[28] M. Warner, Phys. Rev. E **67**, 011701 (2003).
[29] C. M. Stafford, S. Guo, C. Harrison, and M. Y. M. Chiang, Rev. Sci. Instrum. **76**, 062207 (2005).
[30] S. Nikolov, C.-S. Han, and D. Raabe, Int. J. Solids Struct. **44**, 1582 (2007).
[31] X. Zhang, J. Kun, P. Sharma, and B. Yakobson, J. Mech. Phys. Solids **54**, 2304 (2006).